NANO LETTERS

2007
Vol. 7, No. 8
2383−2388

Selective Tuning of the Electronic Properties of Coaxial Nanocables through Exohedral Doping

Antonio G. Souza Filho,*,† Vincent Meunier,‡ Mauricio Terrones,§ Bobby G. Sumpter,‡ Eduardo B. Barros,|| Federico Villalpando-Páez,⊥ Josue Mendes Filho,† Yoong Ahm Kim,# Hiroyuki Muramatsu,# Takuya Hayashi,# Morinobu Endo,# and Mildred S. Dresselhaus▽

Departamento de Física, Universidade Federal do Ceara, P.O. Box 6030, 60455-900 Fortaleza-CE, Brazil, Computer Science and Mathematics Division and Center for Nanophase Materials Sciences, Oak Ridge National Laboratory, Bethel Valley Road, Oak Ridge, Tennessee 37922, Advanced Materials Department, IPICyT, Camino a la Presa San Jose 2055, 78216 San Luis Potosi, SLP, Mexico, Physics Department, Tohoku University, Sendai Japan, Department of Materials Science and Engineering, Massachusetts Institute of Technology, Cambridge, Massachusetts 02139-4307, Faculty of Engineering, Shinshu University, 4-17-1 Wakasato, Nagano-shi 380-8553, Japan, and Department of Physics and Department of Electrical Engineering and Computer Science, Massachusetts Institute of Technology, Cambridge, Massachusetts 02139-4307

Received May 2, 2007

ABSTRACT

The electronic properties of exohedrally doped double-walled carbon nanotubes (DWNTs) have been investigated using density functional theory and resonance Raman spectroscopy (RRS) measurements. First-principles calculations elucidate the effects of exohedral doping on the M@S and S@M systems, where a metallic (M) tube is either inside or outside a semiconducting (S) one. The results demonstrate that metallic nanotubes are extremely sensitive to doping even when they are inner tubes, in sharp contrast to semiconducting nanotubes, which are not affected by doping when the outer shell is a metallic nanotube (screening effects). The theoretical predictions are in agreement with RRS data on Br_2- and H_2SO_4-doped DWNTs. These results pave the way to novel nanoscale electronics via exohedral doping.

Introduction. Carbon nanotubes exhibit remarkable electronic and mechanical properties depending on their chirality and diameter. Although significant efforts have been devoted to the study of single- and multiwalled carbon nanotubes (SWNTs and MWNTs, respectively), only recently has there been an increase in interest in double-walled carbon nanotubes (DWNTs), which can be considered as a hybrid structure lying between SWNTs and MWNTs. DWNTs contain two concentric tubes, and the diameter of the outermost tube is often close to that of SWNTs grown under similar conditions. Quantum confinement effects are expected to play a major role on the inner tubes when the diameters are small (<1 nm).[1] Recent advances in the synthesis of DWNTs have allowed the production of highly crystalline and pure coaxial tubes containing a negligible amount (<1%) of SWNTs and other impurities.[2] These DWNT systems are believed to have the desired properties of cylindrical molecular capacitors, GHz oscillators, nanocomposites, field emission sources, nanotube bi-cables, electronic devices, and other applications.[3−5]

It is well-established that doped nanotubes can be more efficient for several types of applications when compared to their undoped counterparts. They are especially promising for developing diverse applications such as electronic, biomedical devices, composites, and catalysts. One key issue that needs to be addressed, before further developments of doped DWNTs for specific applications, is an understanding of charge-transfer effects between the exohedral dopants and the coaxial tubules, specifically for elucidating the effects of external doping on the inner and outer shells. Such studies

* Corresponding author. E-mail: agsf@fisica.ufc.br.
† Departamento de Física, Universidade Federal do Ceara.
‡ Computer Science and Mathematic Division and Center for Nanophase Materials Sciences, Oak Ridge National Laboratory.
§ Advanced Materials Department, IPICyT.
|| Physics Department, Tohoku University.
⊥ Department of Materials Science and Engineering, Massachusetts Institute of Technology.
Faculty of Engineering, Shinshu University.
▽ gDepartment of Physics and Department of Electrical Engineering and Computer Science, Massachusetts Institute of Technology.

10.1021/nl0710351 CCC: $37.00
Published on Web 06/28/2007

are expected to show how to modify the transport properties of the outer shell while preserving the optical properties of the inner tube, thereby creating systems where the inner and outer tubes can be separately controlled.

In this letter, we report on the electronic properties of exohedrally doped DWNTs with acceptor molecules. We find that the charge localization on each of the inner and outer tubes strongly depends on the configuration of the coaxial arrangement of semiconducting and metallic tubes. It is predicted that the metallic tubule is very sensitive to doping effects even when it is enclosed inside a semiconducting shell. Conversely, when the outer shell is metallic, the external electrostatic field is screened by the metallic (M) tube and the inner semiconducting (S) tube is only weakly affected by the chemical doping. Our theoretical findings are supported by resonance Raman scattering data on DWNTs doped with acceptor (Br_2 and H_2SO_4) species. The Raman studies confirm univocally the theoretical conclusions and point out a general trend, independent of the electronegativity of the doping species. These theoretical and experimental results clearly demonstrate that it is possible to control the electronic properties of inner tubes (mainly metallic) via charge transfer so as to produce coaxial nanotube cables with engineered transport properties.

Theoretical Methods. The calculations presented here were performed using the plane-wave density functional theory (DFT) VASP code.[6] The Perdew−Burke−Ernzerhof (PBE) functional was used for the exchange-correlation description.[7,8] Brillouin zone sampling and energy cut-offs were chosen after a careful convergence study for the charge density and total energy. A vacuum region extending 0.6 nm around the outermost tube in the lateral direction was needed to guarantee the absence of image effects on the charge density transfer.

Because chiral nanotubes in general contain a large number of atoms in their unit cell, and because tubes of different chiralities do not usually have a commensurate lattice constant over small length scales, calculations of the electronic properties of DWNTs composed of chiral nanotubes are typically precluded from ab initio approaches.[9] The only case allowing for different combinations of tubes having different diameters and electronic properties (M or S) while keeping the same lattice constant occurs for zigzag nanotubes (*n*,0) (*n*,integer), which can be either metallic (M) or semiconductor (S) (*n* being a multiple of 3 for M tubes or not for S tubes). This choice is further motivated by a recent work, where it was shown that the most stable DWNT systems are likely made up of uniform chiralities.[10] Therefore, in the present work, we focused on DWNTs composed of zigzag nanotubes in different configurations, namely, metallic inner@semiconducting outer (18,0)@(28,0) (the "@" symbol is used throughout this paper) and metallic inner@semiconducting outer (17,0)@(27,0) arranged in a concentric fashion. The tubular coaxial arrays examined in this study correspond to inner and outer radii of 0.665 and 1.057 nm for the (17,0)@(27,0) and 0.704 and 1.096 nm for the (18,0)@(28,0) DWNTs, which leads to 176 and 184 atoms/unit cell, respectively. The chosen diameters are large enough to avoid the type of hybridization that is present in very small diameter systems that exhibit very strong curvature effects.[1]

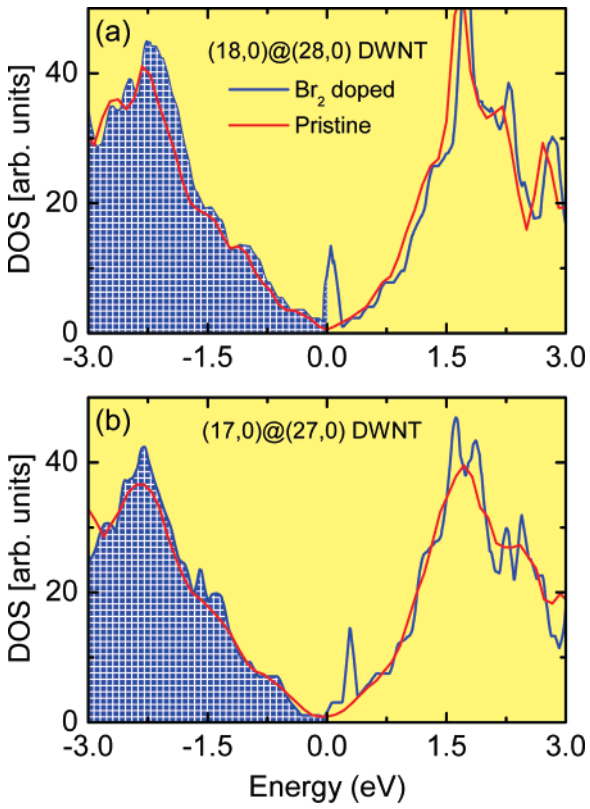

Figure 1. Total calculated density of electronic states (DOS) for DWNT systems. (a) DOS for pristine (red curve) and Br_2-adsorbed (blue curve) of the (18,0)@(28,0) DWNT. (b) The same as in (a) except that the data is for the (17,0)@(27,0) DWNT.

Results. In Figure 1a, we show the total density of electronic states (DOS) calculated for pristine (red curves) and Br_2-adsorbed (blue curves) for the (18,0)@(28,0) DWNT. The zero energy corresponds to the Fermi level. The positions of bromine-doped systems have been relaxed and found to correspond to a shallow (∼40 meV) minimum, typical of a physisorption process, thus indicating that Br_2-doped DWNTs is a typical intercalation compound. This is in agreement with deintercalation experiments where a temperature treatment at 600 °C was shown to be enough for completely removing all of the Br_2 from the DWNT sample and to regain the Raman spectra for the sample before doping, and also for calculations of Br_2 interacting with SWNTs.[11,12] One can observe that the DOS of a pristine DWNT is composed of broad peaks that originate from the hybridizations between the bands of each tube individually. For pristine DWNTs, there is a finite DOS at the Fermi level indicating that the (18,0)@(28,0) DWNT is a metallic system (Figure 1a). When Br_2 is adsorbed on the surface of the outer tube, the DOS near the Fermi level is significantly affected (Figure 1a). The bromine-derived peak is identified with Br_2 states with a very low dispersion when compared to the bands of undoped nanotubes (see Supporting Information), and our calculations show that this sharp peak is partially occupied near the Fermi level. The weak dispersion of the electronic level is partially due to the short lattice constant along the main DWNT axis

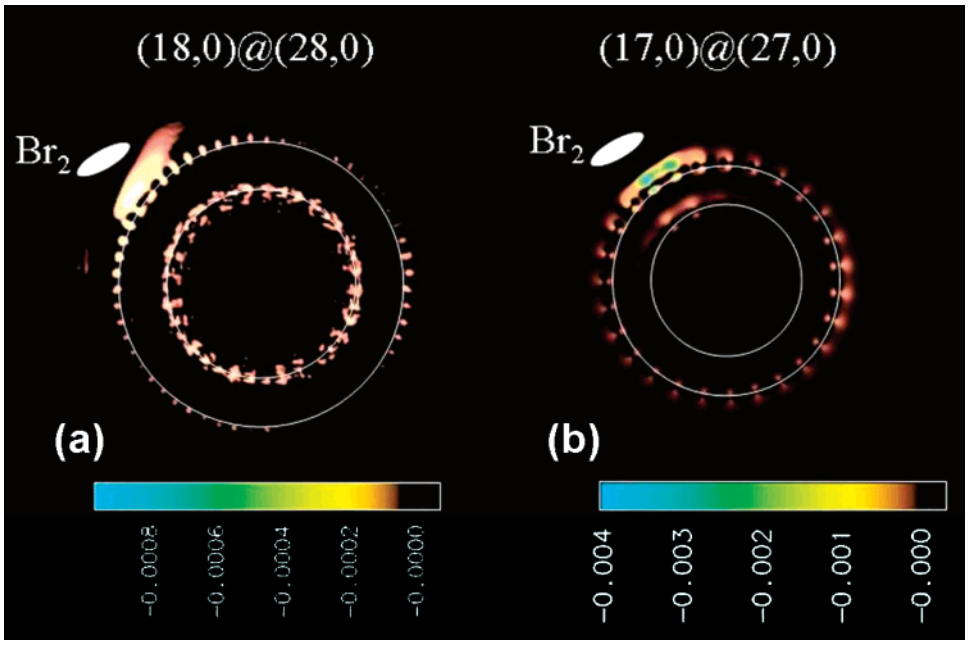

Figure 2. Calculated electronic charge density difference ($\rho_{doped} - \rho_{undoped}$) of Br_2-doped DWNTs. (a) Electronic charge density of Br_2-doped (18,0)@(28,0) DWNTs sitting on a plane perpendicular to the DWNT tube axis. (b) Same as in (a) except that the data is for (17,0)@(27,0) DWNTs. The charge density at the position close to Br_2 has been saturated. The white circles refer to the carbon nanotube cross sections and the white ellipse is the position of Br_2. The lower panels give the ranges of charge density differences for the two figures.

(0.426 nm) and due to some hybridization with the nanotube itself, although the latter effect is rather small, as shown from a comparison between the doped and undoped cases.

Figure 1b shows the calculated DOS of the pristine and Br_2-adsorbed (17,0)@(27,0) DWNT, which is qualitatively similar to that for the (18,0)@(28,0) DWNT except for a smaller shift of the chemical potential (~0.07 eV), and the peak related to the Br_2 states is shifted into the region of the unoccupied bands. The reason for a smaller shift of the Fermi energy is that there are more states available per unit of energy on the metallic tube (27,0) than on the corresponding metallic (18,0) tube of the M@S system shown in Figure 1a. In addition, our calculations demonstrate that bands from the (27,0) tube do hybridize more readily with the bromine states, leading to a larger charge transfer. Because the band gap of a pristine (28,0) tube is about 0.6 eV, the result in Figure 1b indicates that very little net spillover of charge occurs on the semiconducting tube.

This effect can be further investigated by examining the spatial distribution of the electronic charge density plots on the doped DWNTs. In Figure 2, we display a plot of the electronic charge density difference ($\rho_{doped} - \rho_{undoped}$) on a plane perpendicular to the (a) (18,0)@(28,0) and (b) (17,0)@(27,0) nanotube pairs. The plotted charge difference shows the extra holes located in the system after doping. For the (18,0)@(28,0) DWNT, there is a clear delocalization of charges (holes) onto the nanotube systems and a charge redistribution on the semiconductor tube. A net transfer of charge occurs primarily on the inner metallic tube. This result is in clear contrast with the charge distribution for the (17,0)@(27,0) pair, as shown in Figure 2b, where there is very little spillover of charge onto the inner tube and most of the charge (holes) is located around the outer metallic shell. This indicates that the inner semiconducting tube for the (17,0)@(27,0) DWNT is weakly affected by the presence of the exohedral doping.

To support our theoretical predictions, we carried out resonance Raman scattering (RRS) experiments on doped DWNTs with different species (Br_2 and H_2SO_4). The experimental results obtained with RRS are suitable for such comparisons because the Raman spectral profiles are very sensitive to charge-transfer effects.[13] Furthermore, by using the diameter selective resonance Raman effect, it is possible to clearly identify the outer/inner configuration that is being probed for a given laser excitation. It should be pointed out that some of the resonant inner and outer tubes observed do not correspond to the same DWNT but from the diameter distribution it is very likely that for a significant portion of the DWNTs in the bundled sample, both the inner and outer tubes from the same DWNTs answer to the same laser excitation energy. Future experiments on isolated DWNTs will address this point.

In Figure 3, we show the experimental G band Raman spectra for Br_2-doped DWNTs excited with different laser lines. The laser lines were selected to probe the metallic outer/semiconducting inner ($E_{laser} = 1.58$ eV) and semiconducting outer/metallic inner ($E_{laser} = 2.33$ eV) configurations, which allows us to confirm the theoretical predictions presented above. The configuration is identified by using the resonant radial breathing mode spectra as described in ref 11. Although both semiconducting and metallic tubes are contributing to the spectra, the G band of undoped DWNTs shown in Figure 3a has a complex line shape, but we can identify the contribution of inner and outer tubes because the splitting ($\Delta\omega = \omega_G^+ - \omega_G^-$) between the G^+ and G^- modes exhibits a different diameter dependence for metallic

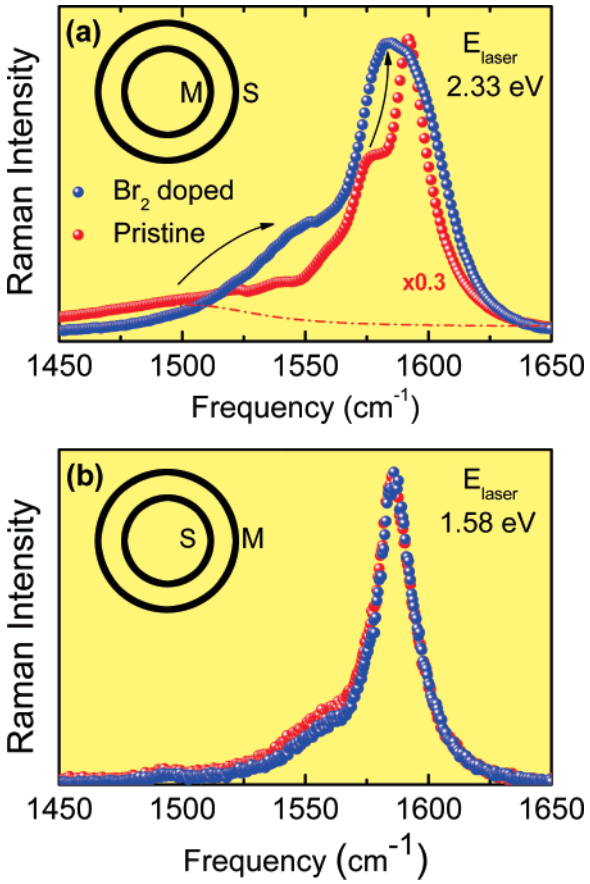

Figure 3. Tangential G-band for pristine and Br_2-doped DWNTs. (a) Experimental G-band Raman profile of pristine (red) and bromine-doped (blue) DWNTs for the metallic inner/semiconductor outer configuration. (b) Same profile as in (a) except for the semiconductor inner/metallic outer configuration. The laser excitation energies used to excite the inner and outer tubes for the two cases are indicated.

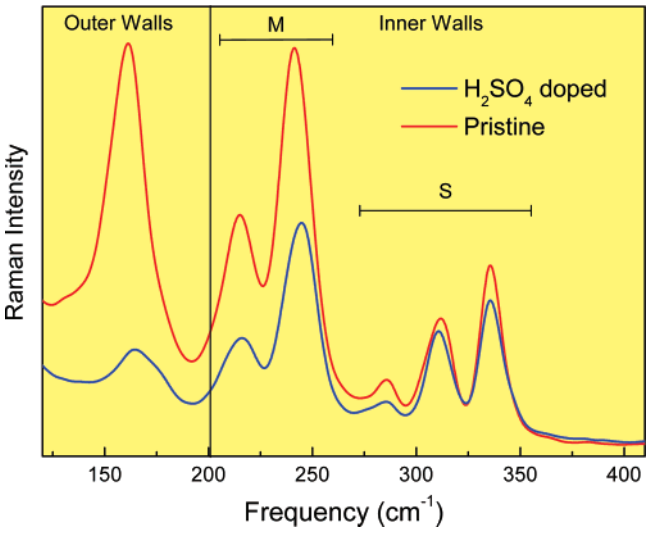

Figure 4. Experimental radial breathing mode Raman profile of pristine (red) and H_2SO_4-doped (blue) DWNTs obtained with $E_{laser} = 2.052$ eV. The resonant inner walls can be either metallic (M) or semiconducting (S) as indicated. The resonant outer shells are semiconducting.

($\Delta\omega = 79.1/d_t^2$) and semiconducting ($\Delta\omega = 47.7/d_t^2$) tubes.[14] The average diameter of both the inner and outer tubes is easily identified in the RBM spectra and the splitting defined above is easily tracked experimentally. We can thus observe that, for the pristine sample, there is a weak and broad Breit−Wigner−Fano (BWF) tail peaked at about 1485 cm^{-1} (dot−dash line in Figure 3a). This BWF tail in the Raman line shape is typical of small diameter metallic tubes and originates from the inner tubes that are metallic.[14] The large splitting $\Delta\omega = \omega_G^+ - \omega_G^- \sim 100$ cm^{-1} is consistent with the average diameter of the inner metallic tubes as measured by their RBM spectra. After Br_2 doping, the experimental G band profile is significantly modified. First, we observe a considerable line broadening, which suggests that contributions from metallic and semiconducting tubes are affected differently by the doping. It is clear that, for the pristine undoped sample, the BWF peak due to the metallic inner tube is identified and it does not overlap with the modes of the outer semiconducting tube because of their very different $\Delta\omega = \omega_G^+ - \omega_G^-$ discussed above. We note that the BWF profile for the inner tube is strongly affected by the Br_2 adsorption. Its frequency exhibits a large upshift from 1485 up to 1545 cm^{-1} (see arrow Figure 3a). Strikingly, when the sample is doped with Br_2, the G^- component is upshifted in frequency, thus indicating extra holes on the nanotubes. Furthermore, the peak at 1575 cm^{-1} in the undoped sample (attributed to the semiconducting outer tubes) also experiences an usphift in frequency (see arrow in Figure 3a), indicating that semiconducting outer tubes are also being affected by the doping in agreement with theoretical predictions. These up shifts are related to a direct electron charge-transfer process from the nanotube to the acceptor Br_2 molecules. These results indicate that metallic nanotubes are very sensitive to doping even when they are surrounded by a semiconducting tube. The observed behavior is in full agreement with the theoretical predictions discussed above for the (18,0)@(28,0) DWNT.

Turning to the S@M system, we show a typical G band Raman spectra in Figure 3b taken with $E_{laser} = 1.58$ eV. The profile is typical of semiconducting nanotubes, and after Br_2 doping, there are little or no changes in the G-band spectra regarding frequency and line shape. The absence of frequency shifts is an unambiguous indication that the inner tubes are only weakly affected by the doping when the outer shell is a metallic tube. Again, this observation comes in full agreement with the theoretical prediction made by the ab initio calculations for the (17,0)@(27,0) DWNT.

A similar screening effect was experimentally observed for H_2SO_4-adsorbed DWNTs.[15] These experiments were performed with highly concentrated sulfuric acid, and because the samples present a high degree of crystallinity, the acid did not attack the nanotube surface structure. The lack of defect formation by H_2SO_4 doping was confirmed by the very weak D band intensity in the Raman spectra of H_2SO_4-treated DWNTs.[15] Another aspect of the effect of exohedral doping is illustrated in Figure 4, which shows the radial breathing mode spectral region for both pristine and H_2SO_4-treated DWNTs. For the laser excitation 2.052 eV, the resonant inner shells are metallic for the larger diameter (smaller RBM frequency) tubes and semiconducting for those

with smaller diameters (larger RBM frequency). Here, the outer shell can also be either semiconducting or metallic tube. In this case, we obtain information on both S@S and M@S. However, regardless of the conductive behavior of the outer shell, we can observe that only the metallic inner nanotubes showed a large decrease in RBM intensity after the acid treatment. In contrast, the intensity and line shape of the RBM feature for the semiconducting inner wall tubes are only slightly affected by H_2SO_4 adsorption in comparison with metallic inner tubes.[15] The changes observed in the semiconducting inner tube behaviors should come from those S tubes that are encapsulated inside a semiconducting tube.

The metallic screening effects discussed in the theoretical modeling (Br_2-doped DWNTs) and experimental data (Br_2- and H_2SO_4-doped DWNTs) were also predicted for B adsorbed (predicted to be an electron donor) on DWNTs, thus pointing out a general trend independent of the electronegativity of the dopant. The experimental data scenario for discussing charge transfer in B-doped DWNTs is more complex because, besides the adsorption (exohedral doping), B atoms can also substitutionally dope (in-plane doping) the nanotube wall. These results will be published in a forthcoming paper.

Finally, we comment on the opportunities opened up by this study relevant to future work on how to further understand the DWNT system itself and the intercalation process in carbon nanotube-based systems. DWNTs have been described as a system where the inner shell is sheltered and free of environmental effects. Very small linewidths have been reported for the Raman modes for the inner tubes in support of this statement.[16] There are also reports in the literature pointing to the presence of the inner−outer shell interaction leading to the metallicity of DWNTs.[17] In particular, the decrease in photoluminescence efficiency of the inner tubes in peapod-derived DWNTs relative to SWNTs with similar diameters has been attributed to the inner−outer shell interaction.[18] The exohedral chemical doping provides a sensitive probe of these effects because it allows a comparative examination to be made of the M@S and S@M inner@outer wall configurations. Intercalation in carbon nanotube bundled samples is different from graphite because of curvature and metallicity effects. It is clear from the experimental results we have discussed here that the inner tubes are not completely free of environmental effects and their conductive behavior configuration is a key factor for defining their doping states. The abundance of metallic inner tubes in our samples is quite unique and it is typical of DWNT samples prepared via the CVD method.[2] Thus, it was possible to access the observed effects reported here because our DWNT sample is substantially different from those derived from the peapod route for which the majority of inner tubes are semiconducting.[16,17]

Conclusions. In summary, results from a joint theoretical and experimental study of exohedral chemically doped double-walled carbon nanotubes demonstrate charge-transfer-mediated electronic properties. We have found that, after doping with acceptor molecules, the charge localization is strongly dependent on the configuration of the inner and outer shells of the DWNTs regarding their conductive (metallic or semiconducting) behavior prior to doping. For the metallic inner/semiconducting outer configuration, the inner tube is highly affected by the exohedral doping, allowing one to achieve control of the electronic structure of the inner tube through chemical doping. This result points out that the assumption of the inner tubes being sheltered and completely free of environmental changes is not general. Both theoretical and experimental findings converge to the existence of a real nanoscale coaxial cable with a semiconducting inner tube screened by a metallic outer shell. These coaxial cables are promising for hybrid electronic and optical devices, where the conduction of the outer shell is tuned through doping and the optical properties (such as photoluminescence) of the inner semiconducting tube are preserved.

Acknowledgment. A portion of this research was conducted at the Center for Nanophase Materials Sciences, which is sponsored at Oak Ridge National Laboratory (ORNL) by the Division of Scientific User Facilities, U.S. Department of Energy. V.M. and B.S. acknowledge the Laboratory Directed Research and Development Program of ORNL. This work was supported in part by CONACYT-México grants: 45772 (MT), 41464-Inter American Collaboration (MT), 2004-01-013/SALUD-CONACYT (MT), and PUE-2004-CO2-9 Fondo Mixto de Puebla (MT). A.G.S.F. acknowledge the support from Brazilian agencies FUNCAP (grant 985/03), CNPq (grants 556549/2005-8, 475329/2006-6, 307417/2004-2), Rede Nacional de Pesquisa em Nanotubos de Carbono (CNPq/MCT-Brazil). The NSF-CNPq (grant 491083/2005-0) joint collaboration is also acknowledged. The work at MIT was supported by grant NSF/DMR 04-05538. M.E. acknowledges support from the CLUSTER of the Ministry of Education, Culture, Sports, Science and Technology.

Supporting Information Available: Calculated electronic band structure of Br_2-adsorbed (18,0)@(28,0) and (17,0)@(27,0) DWNTs. This material is available free of charge via the Internet at http://pubs.acs.org.

References

(1) Okada, S.; Oshiyama, A. *Phys. Rev. Lett.* **2003**, *91*, 216801.
(2) Endo, M., M.; Hayashi, T.; Muramatsu, H.; Kim, Y.-A.; Terrones, H.; Terrones, M.; Dresselhaus, M. S. *Nano Lett.* **2004**, *4*, 1451.
(3) Chen, G.; Bandow, S.; Margine, E. R.; Nisoli, C.; Kolmogorov, A. N.; Crespi, V. H.; Gupta, R.; Sumanasekera, G. U.; Eklund, P. C. *Phys. Rev. Lett.* **2003**, *90*, 257403.
(4) Legoas, S. B.; Coluci, V. R.; Braga, S. F.; Coura, P. Z.; Dantas, S. O.; Galvao, D. S. *Phys. Rev. Lett.* **2003**, *90*, 055504.
(5) Endo, M.; Muramatsu, H.; Hayashi, T.; Kim, Y. A.; Terrones, M.; Dresselhaus, M. S. *Nature* **2005**, *433*, 476.
(6) Kresse, G.; Hafner, J. *Phys. Rev. B* **1993**, *47*, 558−561;. Kresse, G.; **1994**, *49*, 14251−14269.
(7) Perdew, J. P.; Burke, K.; Ernzerhof, M. *Phys. Rev. Lett.* **1996**, *77*, 3865−3868.
(8) Generally, all DFT functionals lead to a systematic overestimation of charge transfer, except for long-range excited states where charges are strongly underestimated. Among the different exchange-correlation functionals, the generalized gradient approximation (GGA) functionals have been reported to yield quantitatively better results than local density approximation (LDA) exchange, although with an overestimation of charge due to the incorrect asymptotic decay in the exchange correlation (XC) potential, as shown in Aleman, C.; Curco, D.; Casanovas J. *Phys. Rev. E* **2005**, *72*, 026704.

(9) Lambin, Ph.; Meunier, V.; Rubio, A. *Phys. Rev. B* **2000**, *62*, 5129−5135.
(10) Guo, W. L.; Guo, Y. F. *J. Am. Chem. Soc.* **2007**, *129*, 2730.
(11) Souza Filho, A. G.; Endo, M.; Muramatsu, H.; Hayashi, T.; Kim, Y. A.; Barros, E. B.; Akuzawa, N.; Samsonidze, Ge. G.; Saito, R.; Dresselhaus, M. S. *Phys. Rev. B* **2006**, *73*, 235413.
(12) Jhi, S. H.; Louie, S. G.; Cohen, M. L. *Solid State Commun.* **2002**, *123*, 495−499.
(13) Souza Filho, A. G., Jorio, A., Samsonidze, Ge. G., Dresselhaus, G., Saito, R.; Dresselhaus, M. S. *Nanotechnology* **2003, *14***, 1130−1139.
(14) Jorio, A.; Souza Filho, A. G.; Dresselhaus, G.; Dresselhaus, M. S.; Swan, A. K., Ünlü, M. S.; Goldberg, B. B.; Pimenta, M. A.; Hafner, J. H.; Lieber, C. M.; Saito, R. *Phys. Rev. B* **2002**, *65*, 155412.
(15) Barros, E. B., Son, H.B., Samsonidze, Ge. G., Souza Filho, A. G., Saito, R., Kim, Y. A., Muramatsu, H., Hayashi, T., Endo, M.; Dresselhaus, M. S. *Phys. Rev. B* **2007**, in press.
(16) Pfeiffer, R.; Kuzmany, H.; Kramberger, Ch.; Schaman, C.; Pichler, T.; Kataura, H.; Achiba, Y.; Kurti, J.; Zolyomi, V. *Phys. Rev. Lett.* **2003**, *90*, 225501.
(17) Pfeiffer, R.; Simon, F.; Kuzmany, H.; Popov, V. N.; Zolyomi, V.; Kurti, J. *Phys. Status Sol*idi *B* **2006**, *243*, 3268−3272.
(18) Okazaki, T.; Bandow, S.; Tamura, G.; Fujita, Y.; Iakoubovskii, K.; Kazaoui, S.; Minami, N.; Saito, T.; Suenaga, K.; Iijima, S. *Phys. Rev. B* **2006**, *74*, 153404.

NL0710351